

Modulational instability criteria for coupled nonlinear transmission lines with dispersive elements

E. Kengne,^{1,2,*} S. T. Chui,³ and W. M. Liu¹¹*Beijing National Laboratory for Condensed Matter Physics, Institute of Physics, Chinese Academy of Sciences, Beijing 100080, China*²*Department of Mathematics & Computer Science, Faculty of Science, University of Dschang, P. O. Box 4509, Douala, Republic of Cameroon*³*Bartol Research Institute, University of Delaware, Newark, Delaware 19716, USA*

(Received 6 June 2006; revised manuscript received 3 July 2006; published 18 September 2006)

We investigate the modulational instability of Stokes wave solutions on a system of coupled nonlinear electrical transmission lines with dispersive elements. In the continuum limit, and in suitable scaled coordinates, the voltage on the system is described by the two-dimensional coupled nonlinear Schrödinger equations. The set of coupled nonlinear Schrödinger equations obtained is analyzed via a perturbation approach. No assumption is made on the signs of the relevant coefficients such as the coefficients of nonlinearity and the coupling coefficients. A set of explicit criteria of modulational stability and modulational instability is derived and analyzed. It is numerically shown that the effect of the dispersive elements in the line is to decrease the instability region and the instability growth rate.

DOI: [10.1103/PhysRevE.74.036614](https://doi.org/10.1103/PhysRevE.74.036614)

PACS number(s): 42.65.Tg, 42.25.Bs, 02.60.Cb

I. INTRODUCTION

The nonlinear dispersive propagation of light in an array of linearly coupled optical fibers can be described by the following difference in the partial differential equations (PDE's):

$$i \frac{\partial A_m}{\partial z} - \beta_2 \frac{\partial^2 A_m}{\partial t^2} + 2\gamma |A_m|^2 A_m - \delta(A_{m+1} + A_{m-1} - 2A_m) = 0. \quad (1)$$

Here $m=1, 2, \dots, M$ is the fiber index, t is the retarded time, δ is the linear coupling, β_2 is the group velocity dispersion coefficient, and γ is nonlinearity coefficient [1]. An initial pulse of Gaussian amplitude, injected into an array of $M=15$ fibers at $z=0$, was seen to “collapse” into the central fiber $m_c=8$ with compression ratios of about 6 over distances of 200 m. This effect arises from the fact that Eq. (1) has a continuum limit corresponding to the two-dimensional Schrödinger equation in which “pulse blow-up” can occur. The work presented here is an investigation to see whether similar instabilities arise in the analogous *electrical* system of coupled nonlinear-dispersive transmission lines (NTL's). We are motivated by developments in the theory of nonlinear waves, especially solitons. Solitons are localized pulses that arise in many physical contexts through a balance of nonlinearity and dispersion. Since the 1970s, various investigators have discovered the existence of solitons in nonlinear transmission lines (NLTLs), through both mathematical models and physical experiments.

In Sec. II, we write down the circuit equations governing small-amplitude pulses on systems of NTL's coupled via constant capacitors. After scaling coordinates and taking a continuum limit, we reduce them to a well-known coupled

nonlinear partial system of equations which possesses a traveling-wave solution that can be unstable under linear perturbation. In Sec. III, we first remind the reader of the phenomenon of modulational instability (MI), and then we undertake an analytic study of the linear stability analysis and modulational (in)stability of these Stokes wave solutions of the coupled NLS equations obtained therein; computational analysis of the modulational instability is also done in this section. We summarize our results in Sec. IV.

II. NONLINEAR TRANSMISSION LINE MODEL

In this section, we review two-dimensional discrete transmission line theory with the aim of clarifying the effects of nonlinearity. Continuum equations that accurately model these effects are derived.

Before examining coupled systems, we introduce our notation by means of a single nonlinear-dispersive transmission line, illustrated in Fig. 1 (see Refs. [2,3]). In this line, the dispersive element is the linear capacitance

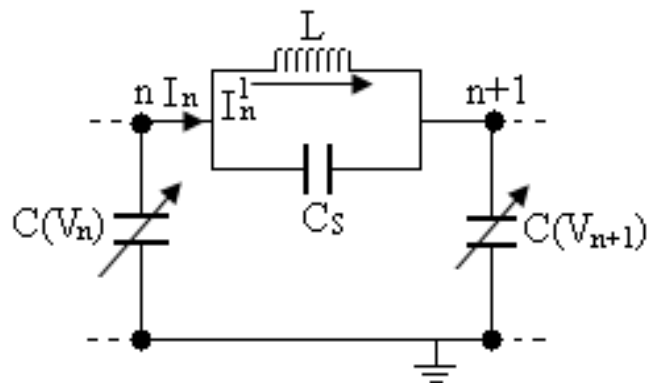


FIG. 1. Part of the system of the nonlinear dispersive transmission line.

*Email address: ekengne6@yahoo.fr

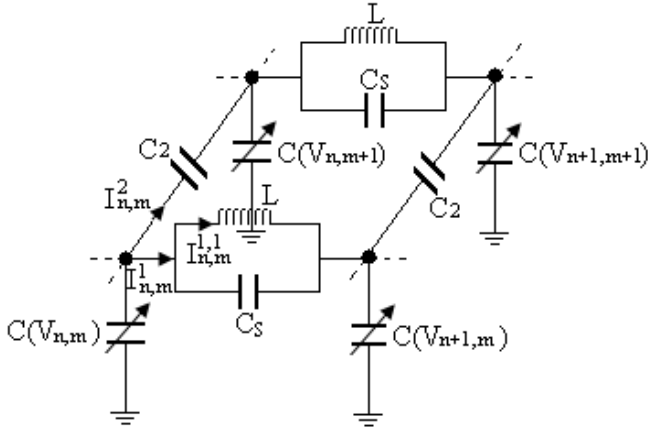


FIG. 2. Part of the system of the nonlinear dispersive transmission line coupled by a capacitor C_2 .

C_S . In this loop, we may write down Kirchoff's laws: $L \frac{\partial I_n^1}{\partial t} = V_{n-1} - V_n$, $I_n - I_n^1 = C_S \frac{\partial}{\partial t} (V_{n-1} - V_n)$, and $\frac{\partial Q_n}{\partial t} = I_n - I_n^1$, where $Q_n \equiv Q(V_n) = \int^{V_n} C(V) dV$ is the charge stored in the n th capacitor. We may use the first two of these equations to eliminate I_n and I_n^1 from the time derivative of the third one. The result is $\frac{\partial^2 Q_n}{\partial t^2} \equiv \frac{\partial}{\partial t} [C(V_n) \frac{\partial V_n}{\partial t}] = C_S \frac{\partial^2}{\partial t^2} (V_{n-1} - 2V_n + V_{n+1}) + \frac{1}{L} (V_{n+1} - 2V_n + V_{n-1})$. This is the circuit equation describing the voltage $V_n(t)$ on a single line.

Now we imagine coupling many identical lines such as this by means of capacitors C_2 at each node. Such a configuration is shown in Fig. 2. The nodes in the system are labeled with two discrete coordinates: n specifies the nodes in the direction of propagation of the pulse, and m labels the lines in the transverse direction. We apply Kirchoff's laws again, this time in orthogonal loops: $L \frac{\partial I_{n,m}^1}{\partial t} = V_{n,m} - V_{n+1,m}$; $I_{n,m}^2 = C_2 \frac{\partial}{\partial t} (V_{n,m} - V_{n,m+1})$, $I_{n,m}^1 - I_{n,m}^{1,1} = C_S \frac{\partial}{\partial t} (V_{n-1,m} - V_{n,m})$, and $\frac{\partial Q_{nm}}{\partial t} = I_{n-1,m}^1 - I_{n,m}^1 + I_{n,m}^2 - I_{n,m}^2$. The circuit equation for this system is therefore

$$\frac{\partial^2 Q_{nm}}{\partial t^2} = \frac{1}{L} (V_{n+1,m} + V_{n-1,m} - 2V_{n,m}) + C_S \frac{\partial^2}{\partial t^2} (V_{n+1,m} + V_{n-1,m} - 2V_{n,m}) + C_2 \frac{\partial^2}{\partial t^2} (V_{n,m+1} + V_{n,m-1} - 2V_{n,m}). \quad (2)$$

In our analysis, we shall take the nonlinear capacitance $C(V_{n,m})$ to be of the form $C(V) = C_0 / (1 + \frac{V}{V_0})$, where C_0 and V_0 are arbitrary capacitance and voltage scales, respectively. In this paper, we only study the case in which the perturbation voltage V is small enough compared to the equilibrium voltage. We then take the continuum limit of Eq. (2) in both the n and m directions, along with the additional provisos that the amplitude of the voltage pulse is small and its wavelength is much greater than the lattice spacings. By treating n and m as continuous variables and V as a function of n , m , and t , and assume that $V \ll V_0$, then Eq. (2) becomes $LC_0 \frac{\partial^2 (V - bV^2)}{\partial t^2} = \frac{\partial^2}{\partial t^2} (V + \frac{1}{12} \frac{\partial^2 V}{\partial n^2} + \dots) + LC_S \frac{\partial^4}{\partial t^2 \partial n^2} (V + \frac{1}{12} \frac{\partial^2 V}{\partial n^2} + \dots) + LC_2 \frac{\partial^4}{\partial t^2 \partial m^2} (V + \frac{1}{12} \frac{\partial^2 V}{\partial m^2} + \dots)$, where $b = \frac{1}{2} V_0$. Next, we transform to "stretched" coordinates that

reflect the fact that the dominant motion is in the n direction: $\xi = \epsilon^{1/2}(n - vt)$, $\eta = \epsilon^{1/2}m$, $\tau = \epsilon^{3/2}t$, and $V = \epsilon u(\xi, \eta, \tau)$, where $\epsilon \ll 1$ is a small parameter. Using these expressions, the above equation becomes, to lowest order in ϵ ,

$$12C_0 b \frac{\partial u^2}{\partial \xi} + \frac{24C_0}{v} \frac{\partial u}{\partial \tau} + (C_0 + 12C_S) \frac{\partial^3 u}{\partial \xi^3} + 12C_2 \frac{\partial^3 u}{\partial \xi \partial \eta^2} = 0, \quad (3)$$

where $v^2 = \frac{1}{LC_0}$ is the linear wave speed.

Let us consider the interaction of any two wave packets centered at (\mathbf{k}_A, ω_A) and (\mathbf{k}_B, ω_B) ; here, \mathbf{k}_j and ω_j are the wave vectors and the frequencies, respectively. In order to resolve the weakly nonlinear equation, two different low time scales $T_1 = \epsilon \tau$ and $T_2 = \epsilon^2 \tau$ must be introduced in addition to the original time scale $T_0 = \tau$. Moreover, we introduce the large spatial scale $X_1 = \epsilon \xi$ and $Y_1 = \epsilon \eta$ in addition to the original $X_0 = \xi$ and $Y_0 = \eta$, where $\epsilon \ll 1$ is a small parameter. Then the voltage in the transmission line is expanded as

$$u = \epsilon u_1 + \epsilon^2 u_2 + \epsilon^3 u_3 + O(\epsilon^4), \quad (4)$$

where $u_j = u_j(X_0, X_1, Y_0, Y_1, T_0, T_1, T_2)$; in Eq. (4) the small parameter ϵ measures the size of the amplitudes of the perturbation. To analyze the propagation of any two wave packets centered around (k_A, ω_A) and (k_B, ω_B) , we take the lowest-order term u_1 in the form

$$u_1 = A \exp[i(\mathbf{k}_A \cdot \mathbf{r} - \omega_A T_0)] + B \exp[i(\mathbf{k}_B \cdot \mathbf{r} - \omega_B T_0)] + \text{c.c.}, \quad (5)$$

where $A = A(X_1, Y_1, T_1, T_2)$, $B = B(X_1, Y_1, T_1, T_2)$ are two complex amplitudes, $\mathbf{r} = (X_0, Y_0)$, and $\mathbf{k}_j = (k_j^{X_0}, k_j^{Y_0})$, so that

$$C_2(C_0 + 12C_S)(k_B^{X_0})^2 - 4C_2^2(k_B^{Y_0})^2 > 0, \quad (6)$$

and c.c. stands for complex conjugate. The carrier wave number \mathbf{k}_j and the frequency ω_j of each wave are related by

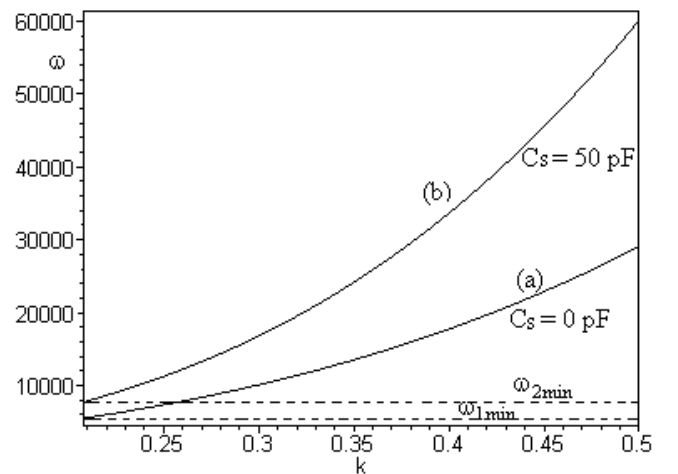


FIG. 3. Linear dispersion curve defined by the dispersion relations in the special case when $k_B^{X_0} = -k_A^{X_0} = k$ and $k_B^{Y_0} = -k_A^{Y_0} = -0.2$ for $k \in [0.12844, 0.2]$. Here we take $L = 200 \mu\text{H}$, $C_0 = 370 \text{ pF}$, $C_2 = 100 \text{ pF}$, $C_S = 0 \text{ pF}$ [for curve (a)] and $C_S = 50 \text{ pF}$ [for curve (b)]. Comparing the two figures, we see that the gap zone is larger in the presence of the linear capacitance C_S .

a dispersion relation function $\omega_j = \omega_j(\mathbf{k}_j)$. As we will show below, nonlinearity is manifested via a slow modulation of the wave amplitudes A and B , in time and space, say, along the x axis and the y axis.

Inserting the perturbation expansions (4) into the nonlinear equation (3) and equating coefficients of like powers of ϵ , we obtain a system of three partial differential equations in u_1 , u_2 , and u_3 . The first of these equations contains only u_1 , the second contains u_1 and u_2 , and the third one contains u_1 , u_2 , and u_3 : $D_0 u_1 = \left[\frac{24C_0}{v} \frac{\partial}{\partial T_0} + (C_0 + 12C_S) \frac{\partial^3}{\partial X_0^3} + 12C_2 \frac{\partial^3}{\partial X_0 \partial Y_0^2} \right] u_1 = 0$, $D_0 u_2 = -\frac{24C_0}{v} \frac{\partial u_1}{\partial T_1} - 3(C_0 + 12C_S) \frac{\partial u_1}{\partial X_0 \partial X_1} - 12C_2 \left(\frac{\partial^2 u_1}{\partial X_1 \partial Y_0^2} + 2 \frac{\partial^2 u_1}{\partial X_0 \partial Y_0 \partial Y_1} \right) - 12C_0 b \frac{\partial u_1^2}{\partial X_0}$, and $D_0 u_3 = -12C_0 b \times \left(2 \frac{\partial u_1 u_2}{\partial X_0} + \frac{\partial u_1^2}{\partial X_1} \right) - \frac{24C_0}{v} \left(\frac{\partial u_2}{\partial T_1} + \frac{\partial u_1}{\partial T_2} \right) - 3(C_0 + 12C_S) \left(\frac{\partial^2 u_2}{\partial X_0 \partial X_1} + \frac{\partial^2 u_1}{\partial X_0 \partial X_1^2} \right) - 12C_2 \left(\frac{\partial^2 u_1}{\partial X_0 \partial Y_1^2} + 2 \frac{\partial^2 u_1}{\partial Y_0 \partial X_1 \partial Y_1} + 2 \frac{\partial^2 u_2}{\partial X_0 \partial Y_0 \partial Y_1} + \frac{\partial^2 u_2}{\partial Y_0^2 \partial X_1} \right)$.

Substituting Eq. (5) in the first equation of the above system leads to the dispersion relations $\frac{24C_0}{v} \omega_j + (C_0 + 12C_S) \times (k_j^{X_0})^3 + 12C_2 k_j^{X_0} (k_j^{Y_0})^2 = 0$, $j=A, B$. In the special case in which $k_B^{X_0} = -k_A^{X_0} = k$ and $k_B^{Y_0} = -k_A^{Y_0} = -0.2$, we plot in Fig. 3 the linear dispersion curve $\omega_B = -\omega_A = \omega(k)$ for the line parameters $L=200 \mu\text{H}$, $C_0=370 \text{ pF}$, $C_2=100 \text{ pF}$, $C_S=0 \text{ pF}$ [for curve (a)], and $C_S=50 \text{ pF}$ [for curve (b)]. For these line parameters, we use Eq. (6) and find that $k > 0.20795$ (for both values of C_S). On these curves, $\omega_{1 \min}$ and $\omega_{2 \min}$ are the values of $\omega(k)$ at $k=0.20796$ and correspond to $C_S=0$ and 50 pF , respectively. Let us denote by $F_{0l} = \frac{\omega_{l \min}}{2\pi}$ ($l=1, 2$) the gap, which is the lower cutoff frequency corresponding to curves (a) and (b). Because $\omega_{1 \min} < \omega_{2 \min}$, we have $F_{01} < F_{02}$. Let $\omega_{1 \max} = \omega(0.5) = 29082$ for curve (a) and $\omega_{2 \max} = \omega(0.5) = 60131$ for curve (b). Then the width of the interval $\left[F_{01}, \frac{\omega_{1 \max}}{2\pi} \right]$ is 3751.7, while that of interval $\left[F_{02}, \frac{\omega_{2 \max}}{2\pi} \right]$ is 8337.8, that is, the width of the interval $\left[F_{01}, \frac{\omega_{1 \max}}{2\pi} \right]$ is smaller than that of interval $\left[F_{02}, \frac{\omega_{2 \max}}{2\pi} \right]$, and hence, introduction of the dispersive element C_S in the line has decreased the propagation domain of the signal. For the future simulations, we use the same line parameters as here.

Since ω_j and \mathbf{k}_j are related by the above dispersion relation, the particular solution of the second equation of the system contains secular terms in either X_0 or T_0 or both, which lead to a nonuniform expansion for either long times or large distances or both. For a uniform expansion, we require the vanishing of terms that produce secular terms. This solvability condition leads to the following equations for A and B :

$$\frac{\partial A}{\partial T_1} = -\frac{\partial \omega_A}{\partial k_A^{X_0}} \frac{\partial A}{\partial X_1} - \frac{\partial \omega_A}{\partial k_A^{Y_0}} \frac{\partial A}{\partial Y_1},$$

$$\frac{\partial B}{\partial T_1} = -\frac{\partial \omega_B}{\partial k_B^{X_0}} \frac{\partial B}{\partial X_1} - \frac{\partial \omega_B}{\partial k_B^{Y_0}} \frac{\partial B}{\partial Y_1}. \quad (7)$$

Eliminating from the third equation of the system the terms that produce secular terms and using Eqs. (6) and (7) lead to

$$i \frac{\partial \psi_j}{\partial \tau} = M_j \nabla^2 \psi_j + (V_{jj} |\psi_j|^2 + V_{j3-j} |\psi_{3-j}|^2 + \mu_j) \psi_j,$$

$$j = 1, 2, \quad (8)$$

where

$$\psi_1 = \psi_1(x, y, \tau) = \epsilon A(x, y, \tau) \exp[-i(\alpha_1 x + \beta_1 y)],$$

$$\psi_2 = \psi_2(x, y, \tau) = \epsilon B \exp[-i(\gamma_1 x + \delta_1 y)],$$

$$\alpha_1 = -\frac{1}{8} \frac{(C_0 + 12C_S) k_A^{X_0} \frac{\partial \omega_A}{\partial k_A^{Y_0}} - 4C_2 k_{Y_0} \frac{\partial \omega_A}{\partial k_A^{X_0}}}{C_2 (C_0 + 12C_S) (k_A^{X_0})^2 - 4C_2^2 (k_A^{Y_0})^2},$$

$$\beta_1 = \frac{1}{2\sqrt{(C_0 + 12C_S) C_2 (k_B^{X_0})^2 - 4C_2^2 (k_B^{Y_0})^2}} \frac{\partial \omega_A}{\partial k_A^{X_0}},$$

$$\gamma_1 = -\frac{1}{8} \frac{(C_0 + 12C_S) k_B^{X_0} \frac{\partial \omega_B}{\partial k_B^{Y_0}} - 4C_2 k_{Y_0} \frac{\partial \omega_B}{\partial k_B^{X_0}}}{C_2 (C_0 + 12C_S) (k_B^{X_0})^2 - 4C_2^2 (k_B^{Y_0})^2},$$

$$\delta_1 = \frac{1}{2\sqrt{(C_0 + 12C_S) C_2 (k_B^{X_0})^2 - 4C_2^2 (k_B^{Y_0})^2}} \frac{\partial \omega_B}{\partial k_B^{X_0}},$$

$$M_j = \frac{2(C_0 + 12C_S) C_2 (k_j^{X_0})^2 - 8C_2^2 (k_j^{Y_0})^2}{(C_0 + 12C_S) k_j^{X_0}},$$

$$V_{jj} = \frac{3C_0 v^2 b^2 (k_j^{X_0})^2}{12C_0 \omega_j + 2v (k_j^{X_0})^2 (C_0 + 12C_S) + 24v C_2 k_j^{X_0} (k_j^{Y_0})^2},$$

$$V_{j3-j} = \frac{v \gamma b k_j^{X_0}}{2}, \quad \text{with } k_1^{X_0} = k_A^{X_0}, k_2^{X_0} = k_B^{X_0},$$

$$\gamma = 24C_0 b (k_A^{X_0} + k_B^{X_0}) \left[12(k_A^{X_0} + k_B^{X_0})(k_A^{Y_0} + k_B^{Y_0})^2 C_2 + (\omega_A + \omega_B) \frac{24C_0}{v} + (k_A^{X_0} + k_B^{X_0})^3 (C_0 + 12C_S) \right]^{-1}$$

$$+ 24C_0 b v (k_A^{X_0} - k_B^{X_0}) [v(C_0 + 12C_S)(k_A^{X_0} - k_B^{X_0})^3 + 24(\omega_A - \omega_B) C_0 + 12C_2 v (k_A^{X_0} - k_B^{X_0}) \times (k_A^{Y_0} - k_B^{Y_0})^2]^{-1},$$

$$\mu_1 = 2 \frac{\sqrt{(C_0 + 12C_S) C_2 (k_A^{X_0})^2 - 4C_2^2 (k_A^{Y_0})^2}}{(C_0 + 12C_S) k_A^{X_0}} \frac{\partial \omega_A}{\partial k_A^{X_0}} \beta_1$$

$$- \frac{1}{2} \left(\frac{\partial \omega_A}{\partial k_A^{Y_0}} - \frac{\partial \omega_A}{\partial k_A^{X_0}} \frac{4C_2 k_A^{Y_0}}{(C_0 + 12C_S) k_A^{X_0}} \right) \alpha_1$$

$$- 2 \frac{[(C_0 + 12C_S) C_2 (k_A^{X_0})^2 - 4C_2^2 (k_A^{Y_0})^2]}{(\alpha_1^2 + \beta_1^2)^{-1} (C_0 + 12C_S) k_A^{X_0}},$$

$$\begin{aligned} \mu_2 &= 2 \frac{\sqrt{(C_0 + 12C_S)C_2(k_B^{X_0})^2 - 4C_2^2(k_B^{Y_0})^2}}{(C_0 + 12C_S)k_B^{X_0}} \frac{\partial \omega_B}{\partial k_B^{X_0}} \delta_1 \\ &\quad - \frac{1}{2} \left(\frac{\partial \omega_B}{\partial k_B^{Y_0}} - \frac{\partial \omega_B}{\partial k_B^{X_0}} \frac{4C_2 k_B^{Y_0}}{(C_0 + 12C_S)k_B^{X_0}} \right) \gamma_1 \\ &\quad - 2 \frac{[(C_0 + 12C_S)C_2(k_B^{X_0})^2 - 4C_2^2(k_B^{Y_0})^2]}{(\gamma_1^2 + \delta_1^2)^{-1}(C_0 + 12C_S)k_B^{X_0}}, \\ x &= \frac{4C_2 k_B^{Y_0}}{(C_0 + 12C_S)k_B^{X_0}} \xi - \eta, \\ y &= \frac{2\sqrt{(C_0 + 12C_S)C_2(k_B^{X_0})^2 - 4C_2^2(k_B^{Y_0})^2}}{(C_0 + 12C_S)k_B^{X_0}} \xi, \end{aligned}$$

and $\nabla^2 = \frac{\partial^2}{\partial x^2} + \frac{\partial^2}{\partial y^2}$ is the Laplace operator (a two-dimensional Cartesian geometry is considered for clarity). Here, $C_2 \neq 0$.

In the case of a single nonlinear transmission line ($C_2 = 0$), we have

$$\begin{aligned} i \frac{\partial \phi_j}{\partial T} &= -\frac{1}{2} \frac{\partial^2 \phi_j}{\partial \xi^2} - \frac{4\tilde{\gamma}C_0 b}{(C_0 + 12C_S)} \left(\frac{\alpha_j}{\tilde{\gamma}} |\phi_j|^2 + |\phi_l|^2 \right) \phi_j, \\ j, l &= A, B, j \neq l, \end{aligned} \quad (9)$$

where $\phi_j = \epsilon_j$, $\alpha_j = 6v k_j^{X_0} C_0 b [24v C_2 k_j^{X_0} (k_j^{Y_0})^2 + 12C_0 \omega_j + 2v (k_j^{X_0})^2 (C_0 + 12C_S)]^{-1}$, $j = A, B$, and $T = -\frac{16C_0}{v(C_0 + 12C_S)k_j^{X_0}} \tau$. Here $\tilde{\gamma}$ coincides with the above expression of γ in which we take $C_2 = 0$. We have thus established that the dynamics of any two wave packets in the discrete nonlinear transmission line shown in Figs. 2 and 1 is described by the coupled nonlinear Schrödinger equations (8) and (9), respectively. In these equations, $\psi_j(x, y, \tau)$ and $\phi_j(\xi, T)$ are the complex amplitudes of the signal in the coupled and noncoupled nonlinear transmission lines of Figs. 2 and Fig. 1, respectively.

In Eq. (8), the quantity M_j with sign “-,” that is, $-M_j$, is the group-velocity dispersion, while in Eq. (9), this group-velocity dispersion is $\frac{1}{2} V_{jj}$ and V_{j3-j} in Eq. (8) model carrier self-modulation and wave coupling, respectively. For Eq. (9), they are $-\frac{4\tilde{\gamma}C_0 b}{(C_0 + 12C_S)} \frac{\alpha_j}{\tilde{\gamma}}$ and $-\frac{4\tilde{\gamma}C_0 b}{(C_0 + 12C_S)}$, respectively. $\mu_j = \mu_j(\omega_j, \mathbf{k}_j)$ is the growing (gain $= -\mu_{0j} > 0$) complex eigenvalue. In the above set of coefficients, the quantities $\partial \omega_j / \partial k_j^{X_0}$ and $\partial \omega_j / \partial k_j^{Y_0}$ are known as group velocities.

Equations (8) are known as the coupled nonlinear Schrödinger (NLS) equations with cubic nonlinearity [4–7]. These equations act as a mathematical model for a periodically twisted elliptical birefringent fiber [8,9]. If $\mu_1 = \mu_2 = 0$, then under the condition of equality of the nonlinear coefficients, Eqs. (8) become the celebrated integrable Manakov model [10–12]. Equations (8), in the case in which one of $\psi_j = 0$, become the well-known nonlinear Schrödinger equation and appear in a great array of contexts [13], such as for example, in semiconductor electronics [14,15], optics in nonlinear media [16], photonics [17], plasmas [18], fundamental of quantum mechanics [19], dynamics of accelerators

[20], mean-field theory of Bose-Einstein condensates [21], or in biomolecular dynamics [22]. In some of these fields and many others, the NLS equation appears as an asymptotic limit for a slowly varying dispersive wave envelope propagating in a nonlinear medium [23,24].

Systems of the coupled NLS equations have been used to describe motions and interactions of more than one wave envelope in cases in which more than one order parameter is needed to specify the system. The coupled NLS equations, also called the coupled Gross-Pitaevskii (GP) equations in the theory of Bose-Einstein condensate, have been receiving a lot of attention with recent experimental advances in multicomponent Bose-Einstein condensates (BECs) [25–32]. In this case, ψ_j are the wave functions of the condensates, and $m_j = -\hbar / 2M_j > 0$ represents the mass of the j th condensate. According to standard theory, the nonlinearity coefficients $\hbar V_{jj}$ are proportional to the scattering lengths a_j via $\hbar V_{jj} = 4\pi \hbar a_j / m_j = -8\pi a_j M_j$, while the coupling coefficients $\hbar V_{j3-j}$ are related to the mutual interaction scattering lengths a_{j3-j} via $\hbar V_{j3-j} = 2\pi \hbar a_{j3-j} / m_{j3-j}$, where $m_{j3-j} = m_j m_{3-j} / (m_j + m_{3-j})$ is the reduced mass. The (linear) last terms in each equation involve the chemical potential $-\hbar \mu_j$, which corresponds to a ground state of the condensate, in a simplified model. These terms may readily be eliminated via a simple phase-shift transformation; this is, however, deliberately not done at this stage, for generality. Nevertheless, one therefore intuitively expects no major influence of the chemical potentials on the coupled BEC dynamics (at least for the physical problem studied here).

Equations (9) can be derived from Hamiltonian $H = \int_{-\infty}^{+\infty} \left\{ \left| \frac{\partial \phi_A}{\partial \chi} \right|^2 + \left| \frac{\partial \phi_B}{\partial \chi} \right|^2 - \frac{8C_0 b \gamma}{(C_0 + 12C_S)} \left| \phi_A \right|^2 \left| \phi_B \right|^2 - \frac{2C_0 b (\alpha_A + \alpha_B)}{(C_0 + 12C_S)} \times (|\phi_A|^4 + |\phi_B|^4) \right\} d\chi$, which is a dynamical invariant of the model ($dH/d\tau = 0$). In addition, Eqs. (9) conserve the momentum, $P = i \int_{-\infty}^{+\infty} \left(\phi_A^* \frac{\partial \phi_1}{\partial \chi} + \phi_B^* \frac{\partial \phi_2}{\partial \chi} \right) d\chi$, where * stands for the complex conjugate. Equations (9) are tantamount to those describing light transmission in bimodal nonlinear optical fibers, with two modes representing either different wavelengths or two orthogonal polarizations [6]. The two nonlinear terms in Eqs. (9) account for, respectively, the SPM and XPM (self- and cross-phase-modulation) interactions of two waves.

In the case in which one of ψ_j is zero, Eq. (9) becomes a one-component nonlinear Schrödinger equation that is of major importance in continuum mechanics, plasma physics, nonlinear optics, and condensed matter [where it describes the behavior of a weakly interacting Bose gas and is known as the Gross-Pitaevskii (GP) equation]. The reason for its importance and ubiquity is that it describes the evolution of the envelope ψ of an almost monochromatic wave in a conservative system of weakly nonlinear dispersive waves.

With the above line parameters and the above special case ($k_B^{X_0} = -k_A^{X_0} = -k$, $k_B^{Y_0} = -k_A^{Y_0} = -q$), the dispersion coefficients M_j are depicted in Fig. 4 with $q = 0.2$ in the range $0.12844 \leq k \leq 1.5$. The minimal value of k is obtained from condition (6). The dispersion coefficient curves show that the dispersion coefficient M_1 decreases with the presence of the linear constant capacitance C_S , while the dispersion coefficient M_2 increases with the introduction of C_S in the line.

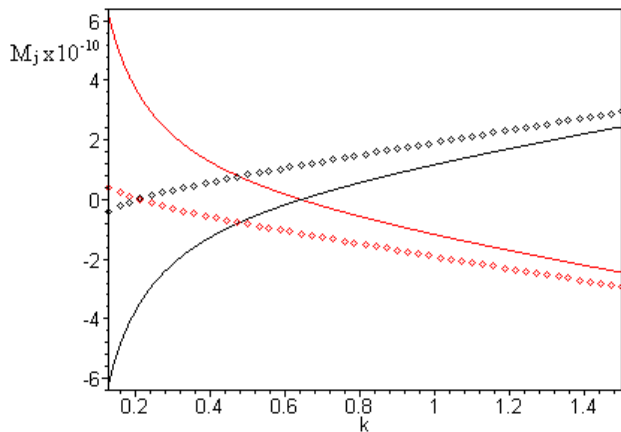


FIG. 4. (Color online) Dispersion coefficients in terms of the wave number k taken from condition (6). The black curves are the M_1 curve, while the red curves are the M_2 curve. The dashed lines correspond to $C_S=0$ and the solid lines correspond to $C_S=50$ pF, $0.12844 \leq k \leq 1.5$. The parameter lines are the same as above. These curves show that the dispersive coefficients M_j take both positive and negative values and inform that the dispersion coefficient M_1 (M_2) decreases (increases) with the introduction of the linear constant capacitance C_S in the line.

III. LINEAR STABILITY ANALYSIS AND MODULATIONAL INSTABILITY (MI) CRITERIA

Modulational instability (MI) by which a plane wave breaks up into filaments at high intensities is a ubiquitous process that occurs in many branches of physics [33]. Over the years, MI has been observed in various physical settings, including hydrodynamics [34,35], plasma physics [36], nonlinear optics [37,38], and quite recently in Bose-Einstein condensates [39]. MI is the outcome of the interplay between nonlinearity and dispersive and/or diffraction effects. It is a symmetry-breaking instability so that a small perturbation on top of a constant amplitude background experiences exponential growth, and this leads to beam breakup in either space or time. Since this disintegration typically occurs in the same parameter region where bright solitons are observed, MI is considered, to some extent, a precursor to soliton formation [40]. Modulational instability is responsible for the formation of envelope solitons in electrical transmission lines [3,43]. MI also sets a fundamental nonlinear limiting factor in the transmission of dense wavelength-division multiplexed signals in long-distance electrical links. The phenomenon of the MI in a homogeneous medium has been extensively studied for scalar and vector nonlinear Schrödinger equations [6,41,42] and its criteria for multi-component BECs have been obtained [44–47]. It has been shown that MI depends on the frequencies of initial modulations and the powers of waves [42]. All these results were obtained in media where the characteristic parameters are constant. In realistic multiconnected electric transmission links, the chromatic dispersion and nonlinearity are not constant but can fluctuate stochastically around their mean values. The inhomogeneity of the medium may be inherent to

the medium or induced by other propagating waves. The situation is relevant for electrical cables where all characteristic parameters fluctuate slightly around their mean values. Note that MI is an important nonlinear limiting factor in long-distance multiconnected electric circuits, but it is also a way to generate a train of solitonlike pulses. Indeed, when a small modulation is applied to an input signal (current or voltage), MI can be induced if the side band frequency falls within the MI gain spectrum. If we make use of this induced MI, it is possible to generate a train of solitonlike pulses with a repetition frequency determined by the inverse of the input modulation frequency. In order to produce the desired pulse train, it is necessary to remove the pulse train at an appropriate distance that is very sensitive to the MI gain at frequency [5–8]. To our knowledge, there are not many works that have studied the phenomenon of MI using a coupled nonlinear transmission line with dispersive element.

In this section, we find the conditions under which a uniform wave train moving along the coupled discrete nonlinear electrical transmission line shown in Fig. 2 will become stable on unstable to a small perturbation. We start with linear stability analysis.

A. Linear stability analysis

We first seek a Stokes wave solutions in the form $\psi_j(x, y, \tau) = \psi_{j0} \exp[i(k_{0j}x + q_{0j}y + \varphi_j(\tau))]$, where ψ_{j0} is a (constant real) amplitude, $\varphi_j(\tau)$ is a (real) phase, and k_{0j} and q_{0j} are (real) wave numbers of the carrier waves, into the coupled nonlinear Schrödinger equations (8). Inserting this expression into Eqs. (8), we find the Stokes wave solutions in the form $\varphi_j(\tau) = \Omega_{j0}\tau$, where $\Omega_{j0} = M(k_{0j}^2 + q_{0j}^2) - (V_{jj}\psi_{j0}^2 + V_{j3-j}\psi_{j0}^2 + \mu_j)$ is the frequency of the carrier waves, $j=1, 2$.

Let us consider a small perturbation around the stationary state $\psi_j = \psi_{j0} \exp[-i(V_{jj}\psi_{j0}^2 + V_{j3-j}\psi_{j0}^2 + \mu_j)\tau]$ by taking $\psi_j = (\psi_{j0} + \varepsilon\psi_{j1}) \exp[i\varphi_j(\tau)]$, where $\psi_{j1}(x, y, \tau)$ is a complex function denoting the small ($\varepsilon \ll 1$) perturbation of the slowly varying modulated complex amplitude (it includes both amplitude and phase corrections), and $\varphi_j(\tau) = \Omega_{j0}\tau$ is the above phasor. Substituting into Eqs (8) and separating into real and imaginary parts by writing $\psi_{j1} = a_j + ib_j$, the first-order terms (in ε) yield $\frac{\partial b_j}{\partial \tau} = -M_j \Delta a_j - 2V_{jj}\psi_{j0}^2 a_j - 2V_{jl}\psi_{j0}\psi_{l0} a_l$, $\frac{\partial a_j}{\partial \tau} = M_j \Delta b_j$, where j and l ($l \neq j$) = 1, 2 (this will henceforth be assumed unless otherwise stated). Eliminating b_j , these equations yield

$$\frac{\partial^2 a_j}{\partial \tau^2} = -M_j \Delta (M_j \Delta a_j + 2V_{jj}\psi_{j0}^2 a_j) - 2V_{jl}\psi_{3-j0}\psi_{j0} \Delta a_{3-j},$$

$$j = 1, 2. \quad (10)$$

Now, we let $a_j = a_{j0} \exp[i(Kx + Qy - \Omega_k \tau)] + \text{complex conjugate}$, where $\mathbf{k} = (K, Q)$ and Ω_k are the wave number and the frequency of low-frequency perturbations modulating the carrier signal, respectively, and a_{j0} is a (constant) complex amplitude. Ω_k is the growth rate. For the determination of a_{j0} , we insert the expression of a_j into Eq. (10) and obtain the linear algebraic

system $(2M_j V_{11} \psi_{10}^2 \mathbf{k}^2 - M_j^2 \mathbf{k}^4 + \Omega_k^2) a_{10} + 2M_j V_{12} \psi_{10} \psi_{20} \mathbf{k}^2 a_{20} = 0$, $2M_j V_{21} \psi_{20} \psi_{10} \mathbf{k}^2 a_{10} + (2M_j V_{22} \psi_{20}^2 \mathbf{k}^2 - M_j^2 \mathbf{k}^4 + \Omega_k^2) a_{20} = 0$, where $\mathbf{k}^2 = \mathbf{k} \cdot \mathbf{k} = K^2 + Q^2$. For a nontrivial solution, the determinant of the coefficients matrix of this system must vanish. That is, the frequency Ω_k and the wave number $\mathbf{k} = (K, Q)$ must be related by the dispersion relation

$$\begin{aligned} & \left(\Omega_k^2 + (M_1 V_{11} \psi_{10}^2 + M_2 V_{22} \psi_{20}^2) \mathbf{k}^2 - \frac{M_1^2 + M_2^2}{2} \mathbf{k}^4 \right)^2 \\ &= \mathbf{k}^4 \left[\left(\frac{M_2^2 - M_1^2}{2} \mathbf{k}^2 + M_1 V_{11} \psi_{10}^2 - M_2 V_{22} \psi_{20}^2 \right)^2 \right. \\ & \quad \left. + 4V_{12} V_{21} M_1 M_2 \psi_{10}^2 \psi_{20}^2 \right]. \end{aligned} \quad (11)$$

We stress that this dispersion relation (which is independent of the chemical potentials or Kerr coefficients μ_j) relies on absolutely no assumption on the sign or the magnitude of $\hbar M_j$, $\hbar V_{jj}$, and $\hbar V_{j3-j}$.

B. Modulational instability criteria for coupled nonlinear transmission lines

The phenomenon of the MI is observed when the angular frequency $\Omega_k = \Omega_k(\mathbf{k})$ of the perturbation functions has a non-zero imaginary part leading to an exponential growth of the amplitude versus time. The dispersion relation (11) takes the form of a bi-quadratic polynomial equation and has the solutions

$$\begin{aligned} \Omega_{k\pm}^2 &= \mathbf{k}^2 \left[\frac{M_1^2 + M_2^2}{2} \mathbf{k}^2 - (M_1 V_{11} \psi_{10}^2 + M_2 V_{22} \psi_{20}^2) \right. \\ & \quad \times \left[\pm \left[\left(\frac{M_2^2 - M_1^2}{2} \mathbf{k}^2 + (M_1 V_{11} \psi_{10}^2 - M_2 V_{22} \psi_{20}^2) \right)^2 \right. \right. \\ & \quad \left. \left. + 4V_{12} V_{21} M_1 M_2 \psi_{10}^2 \psi_{20}^2 \right]^{1/2} \right]. \end{aligned} \quad (12)$$

Equation (12) defines four branches of instability growth rate. We note that the right-hand side of Eq. (11) is real and is either non-negative or negative. Stability is ensured (for any wave vector \mathbf{k}) if (and only if) both solutions $\Omega_{k\pm}^2$ are non-negative. In fact, for a given wave vector \mathbf{k} , the growth rate $\Omega_{k\pm}$ are real, and hence a_1 and a_2 are bounded if, and only if, the right-hand side of Eq. (12) is real. We formulate the results in terms of the following theorem.

Theorem 1. Let $M_1^2 - M_2^2 \neq 0$. In order that $\Omega_{k\pm}^2$ should be non-negative for any wave vector k , it is necessary that either $V_{12} V_{21} M_1 M_2 \geq 0$ or $V_{12} V_{21} M_1 M_2 < 0$ ($M_1 V_{11} \psi_{10}^2 - M_2 V_{22} \psi_{20}^2 > 0$ and $M_1 V_{11} \psi_{10}^2 - M_2 V_{22} \psi_{20}^2 > 0$, and $M_2^2 - M_1^2 > 0$, and sufficient that $M_1 V_{11} \psi_{10}^2 + M_2 V_{22} \psi_{20}^2 \leq 0$, and either $(M_2 V_{11} \psi_{10}^2 - M_1 V_{22} \psi_{20}^2)^2 + 4M_1 M_2 V_{12} V_{21} \psi_{10}^2 \psi_{20}^2 < 0$ or $(M_2 V_{11} \psi_{10}^2 - M_1 V_{22} \psi_{20}^2)^2 + 4M_1 M_2 V_{12} V_{21} \psi_{10}^2 \psi_{20}^2 \geq 0$, $3(M_1 V_{22} \psi_{20}^2 + M_2 V_{11} \psi_{10}^2)^2 + 4M_1 M_2 (V_{11} V_{22} - V_{12} V_{21}) \psi_{10}^2 \psi_{20}^2 > 0$, and $M_1 M_2 (M_1 V_{22} \psi_{20}^2 + M_2 V_{11} \psi_{10}^2) < 0$.

An analysis of this theorem shows that its conditions are satisfied for any perturbation amplitude $|\psi_j|$ as soon as

$M_1 M_2 V_{11} V_{22} > M_1 M_2 V_{12} V_{21} > 0$ and $M_j V_{jj} < 0$. In particular, if $M_j < 0$, then the conditions of theorem 1 are met as soon as $V_{11} V_{22} > V_{12} V_{21} > 0$ and $V_{jj} > 0$.

Theorem 2. Let $M_1^2 - M_2^2 = 0$. In order that $\Omega_{k\pm}^2$ should be non-negative for any wave vector \mathbf{k} , it is necessary that $(M_1 V_{11} \psi_{10}^2 - M_2 V_{22} \psi_{20}^2)^2 + 4M_1 M_2 V_{12} V_{21} \psi_{10}^2 \psi_{20}^2 \geq 0$ and sufficient that $M_1 V_{11} \psi_{10}^2 + M_2 V_{22} \psi_{20}^2 < 0$ and $M_1 M_2 (V_{12} V_{21} - V_{11} V_{22}) < 0$.

After some analyses of theorem 2, we easily see that the conditions of this theorem are valid for any perturbation amplitude $|\psi_j|$ as soon as one of the following conditions is satisfied:

(i) $M_1 = M_2 < 0$, $V_{12} V_{21} > 0$, $V_{jj} > 0$, $V_{12} V_{21} - V_{11} V_{22} < 0$;

(ii) $M_1 = M_2 > 0$, $V_{12} V_{21} > 0$, $V_{jj} < 0$, $V_{12} V_{21} - V_{11} V_{22} < 0$;

(iii) $M_1 = -M_2 > 0$, $V_{12} V_{21} < 0$, $V_{11} < 0$, $V_{22} > 0$, and $V_{11} V_{22} - V_{12} V_{21} < 0$;

(iv) $M_1 = -M_2 < 0$, $V_{12} V_{21} < 0$, $V_{11} > 0$, $V_{22} < 0$, and $V_{11} V_{22} - V_{12} V_{21} < 0$.

We note that if the necessary conditions in theorem 1 are violated, then the right-hand side of Eq. (11) will be negative for any wave vector \mathbf{k} satisfying either condition $\mathbf{k}^2 < 2 \frac{-(M_1 V_{11} \psi_{10}^2 - M_2 V_{22} \psi_{20}^2) \pm 2|\psi_{10} \psi_{20}| \sqrt{-V_{12} V_{21} M_1 M_2}}{M_2^2 - M_1^2}$ or condition $\mathbf{k}^2 > 2 \frac{-(M_1 V_{11} \psi_{10}^2 - M_2 V_{22} \psi_{20}^2) \pm 2|\psi_{10} \psi_{20}| \sqrt{-V_{12} V_{21} M_1 M_2}}{M_2^2 - M_1^2}$. For these wave vectors,

$\Omega_{k\pm}^2$ will be a complex number. In the case of the violation of the necessary conditions in theorem 2, the right-hand side of Eq. (11) will be negative for every wave vector, and then $\Omega_{k\pm}^2$ will always be complex. On the other hand, if the necessary conditions in both theorem 1 and theorem 2 are fulfilled, then the right-hand side of Eq. (12) is real and is either non-negative or negative. In order that both $\Omega_{k\pm}^2$ should be non-negative for any wave vector \mathbf{k} , the sufficient conditions in theorem 1 and theorem 2 must be satisfied. Thus, if the sufficient conditions in either theorem 1 or theorem 2 are violated, then for some values of wave vector, the right-hand side of Eq. (12) will be negative, and then the corresponding $\Omega_{k\pm}$ will be complex, which leads to the modulational instability. It is also possible for $\Omega_{k\pm}^2$ to be complex for any wave vector \mathbf{k} . For example, if $M_2^2 - M_1^2 < 0$, $V_{12} V_{21} M_1 M_2 < 0$, $M_1 V_{11} \psi_{10}^2 - M_2 V_{22} \psi_{20}^2 < 0$, and $(M_1 V_{11} \psi_{10}^2 - M_2 V_{22} \psi_{20}^2)^2 + 4V_{12} V_{21} M_1 M_2 \psi_{10}^2 \psi_{20}^2 > 0$, then the right-hand side of Eq. (11) will be negative for any wave vector \mathbf{k} . Hence, $\Omega_{k\pm}^2$ will be complex for any wave vector \mathbf{k} . This situation also happens when $M_2^2 - M_1^2 = 0$ and $(M_1 V_{11} \psi_{10}^2 - M_2 V_{22} \psi_{20}^2)^2 + 4M_1 M_2 V_{12} V_{21} \psi_{10}^2 \psi_{20}^2 < 0$, because under these conditions, the right-hand side of Eq. (11) will be negative for any wave vector \mathbf{k} , and then $\Omega_{k\pm}^2$ given by Eq. (12) will be complex for every \mathbf{k} . We then obtain the following theorem.

Theorem 3. If either $M_2^2 - M_1^2 < 0$, $V_{12} V_{21} M_1 M_2 < 0$, $M_1 V_{11} \psi_{10}^2 - M_2 V_{22} \psi_{20}^2 < 0$, and $(M_1 V_{11} \psi_{10}^2 - M_2 V_{22} \psi_{20}^2)^2 + 4V_{12} V_{21} M_1 M_2 \psi_{10}^2 \psi_{20}^2 > 0$ or $M_2^2 - M_1^2 = 0$ and $(M_1 V_{11} \psi_{10}^2 - M_2 V_{22} \psi_{20}^2)^2 + 4M_1 M_2 V_{12} V_{21} \psi_{10}^2 \psi_{20}^2 < 0$, then all the $\Omega_{k\pm}^2$ given by Eq. (12) will be complex for any wave vector \mathbf{k} .

Analyzing theorem 3, we find that if $M_2^2 - M_1^2 < 0$, $V_{12} V_{21} M_1 M_2 < 0$, $M_1 V_{11} < 0$, $M_2 V_{22} > 0$, and $M_1 M_2 (2V_{12} V_{21} - V_{11} V_{22}) > 0$, then the conditions of theorem

TABLE I. Coefficients of the coupled NLS equations (8) for different values of the dispersive element C_S for $k_B^{X_0} = -k_A^{X_0} = -0.4$ and for the line parameters (13).

C_S	M_1	M_2	V_{11}	V_{22}	V_{12}	V_{21}
0	0.58378×10^{-10}	-0.58378×10^{-10}	3.0145×10^5	4.0226×10^5	1.2688×10^6	-1.2688×10^6
50	0.71753×10^{-10}	-0.71753×10^{-10}	1.3241×10^5	1.3052×10^5	6.6937×10^5	-6.6937×10^5
100	7.4904×10^{-11}	-7.4904×10^{-11}	84840	77895	4.546×10^5	-4.546×10^5

3 are satisfied for any perturbation amplitude $|\psi_{j0}|$. In particular, for $M_j < 0$, the conditions of theorem 3 will be valid as soon as $M_2^2 - M_1^2 < 0$, $V_{12}V_{21} < 0$, $V_{11} > 0$, $V_{22} < 0$, and $2V_{12}V_{21} - V_{11}V_{22} > 0$.

It is important to note that if the conditions of each of theorems 1, 2, and 3 are violated, then at least one of Ω_{k+}^2 and Ω_{k-}^2 will be positive for some wave vectors \mathbf{k} and the other one will be negative for some other wave vectors \mathbf{k} . For example, let $M_2^2 - M_1^2 = 0$ ($M_1V_{11}\psi_{10}^2 - M_2V_{22}\psi_{20}^2$)² + $4M_1M_2V_{12}V_{21}\psi_{10}^2\psi_{20}^2 \geq 0$. Then if $M_1V_{11}\psi_{10}^2 + M_2V_{22}\psi_{20}^2 < 0$ and $M_1M_2(V_{12}V_{21} - V_{11}V_{22}) > 0$, we will have $\Omega_{k+}^2 \geq 0$ for any \mathbf{k} , and $\Omega_{k+}^2 < 0$ for every wave vector \mathbf{k} , verifying the condition

$$\mathbf{k}^2 < \frac{2}{M_1^2 + M_2^2} [M_1V_{11}\psi_{10}^2 + M_2V_{22}\psi_{20}^2 + \sqrt{(M_1V_{11}\psi_{10}^2 - M_2V_{22}\psi_{20}^2)^2 + 4V_{12}V_{21}M_1M_2\psi_{10}^2\psi_{20}^2}];$$

if the wave vector \mathbf{k} is taken from the condition

$$\mathbf{k}^2 < \frac{2}{M_1^2 + M_2^2} [M_1V_{11}\psi_{10}^2 + M_2V_{22}\psi_{20}^2 + \sqrt{(M_1V_{11}\psi_{10}^2 - M_2V_{22}\psi_{20}^2)^2 + 4V_{12}V_{21}M_1M_2\psi_{10}^2\psi_{20}^2}],$$

then Ω_{k+}^2 will be positive. If $M_1V_{11}\psi_{10}^2 + M_2V_{22}\psi_{20}^2 > 0$ and $M_1M_2(V_{12}V_{21} - V_{11}V_{22}) < 0$, then both $\Omega_{k\pm}^2$ will be positive for any wave vector \mathbf{k} satisfying the condition

$$\mathbf{k}^2 > \frac{2}{M_1^2 + M_2^2} [M_1V_{11}\psi_{10}^2 + M_2V_{22}\psi_{20}^2 + \sqrt{(M_1V_{11}\psi_{10}^2 - M_2V_{22}\psi_{20}^2)^2 + 4V_{12}V_{21}M_1M_2\psi_{10}^2\psi_{20}^2}];$$

both $\Omega_{k\pm}^2$ will be negative for every wave vector \mathbf{k} verifying the condition

$$\mathbf{k}^2 < \frac{2}{M_1^2 + M_2^2} [M_1V_{11}\psi_{10}^2 + M_2V_{22}\psi_{20}^2 - \sqrt{(M_1V_{11}\psi_{10}^2 - M_2V_{22}\psi_{20}^2)^2 + 4V_{12}V_{21}M_1M_2\psi_{10}^2\psi_{20}^2}];$$

for any wave vector \mathbf{k} verifying the condition

$$\begin{aligned} & \frac{2}{M_1^2 + M_2^2} [M_1V_{11}\psi_{10}^2 + M_2V_{22}\psi_{20}^2 + \sqrt{(M_1V_{11}\psi_{10}^2 - M_2V_{22}\psi_{20}^2)^2 + 4V_{12}V_{21}M_1M_2\psi_{10}^2\psi_{20}^2}] \\ & > \mathbf{k}^2 > \frac{2}{M_1^2 + M_2^2} [M_1V_{11}\psi_{10}^2 + M_2V_{22}\psi_{20}^2 - \sqrt{(M_1V_{11}\psi_{10}^2 - M_2V_{22}\psi_{20}^2)^2 + 4V_{12}V_{21}M_1M_2\psi_{10}^2\psi_{20}^2}], \end{aligned}$$

we will have $\Omega_{k+}^2 < 0$ and $\Omega_{k-}^2 > 0$. These two examples show that both $\Omega_{k\pm}^2$ can be positive for some values of wave vector, and negative for some other values of wave vector \mathbf{k} ; also, one of the Ω_{k+}^2 and Ω_{k-}^2 can be positive or negative for all wave vectors \mathbf{k} and the second one changes its sign with different values of k . Hence we get the following theorem.

Theorem 4. If the conditions of each of theorems 1, 2, and 3 are not met, then both $\Omega_{k\pm}^2$ cannot be of the same sign for every wave vector \mathbf{k} .

It is clear that for the complex Ω_{k+} or Ω_{k-} , $a_j = a_{j0} \exp[i(Kx + Qy - \Omega_k \tau)] + \text{complex conjugate}$ with $a_{j0} \neq 0$ will be unbounded, and the modulational instability occurs. We then conclude that theorem 1 and theorem 2 give the criteria of the modulational stability of the Stokes wave solutions $\psi_j = \psi_{j0} \exp[-i(V_{jj}\psi_{j0}^2 + V_{j3-j}\psi_{3-j0}^2 + \mu_j)\tau]$ of system (8), while the criteria of the modulational instability are given by theorem 3.

Because the criteria on the modulational (in)stability we found in this section depend mainly on the coefficients of Eq. (8), which depend only on the parameters of the coupled nonlinear transmission line of Fig. 2 when $k_j^{X_0}$, $k_j^{Y_0}$, and ω_j are given, we conclude that for a given coupled nonlinear transmission line, a modulational instability may or may not occur, depending on the electrical properties of the line.

C. Computational analysis

For all computational simulations, the following nonlinear transmission line parameters are used:

$$C_0 = 370 \text{ pF}, C_2 = 100 \text{ pF}, L = 200 \text{ } \mu\text{H}, V_0 = 2V, \quad (13)$$

$$b = 0.25 \text{ V}^{-1},$$

while the dispersive element C_S is taken variable. For these line parameters, we compute $v = 1/\sqrt{LC_0} = 3.6761 \times 10^6$. Table I gives the coefficients of the couple NLS equations (8) for some values of C_S , when $k_B^{X_0} = -k_A^{X_0} = -0.4$ and $k_B^{Y_0} = -k_A^{Y_0} = -0.2$. Using this table, we compute the frequency square Ω_{k-}^2 and the modulational instability growth $\pm i\Omega_{k-}$ as a function of squared modulation wave function \mathbf{k}^2 . In Fig. 5, the frequency square Ω_{k-}^2 and the typical structure of the modulational instability growth rate $\Gamma = -i\Omega_{k-}(\mathbf{k})$ as functions of squared modulation wave number \mathbf{k}^2 are depicted for the line parameters (13). The amplitudes of the Stokes wave solutions are taken in the proportion $|\psi_{20}|^2 = 2|\psi_{10}|^2 = 10^{-16}$. Figure 5(a) gives the frequency square versus the squared modulation wave number \mathbf{k}^2 . Here, the dotted black line, the solid black line, and the solid red line correspond to $C_S = 0, 50$, and

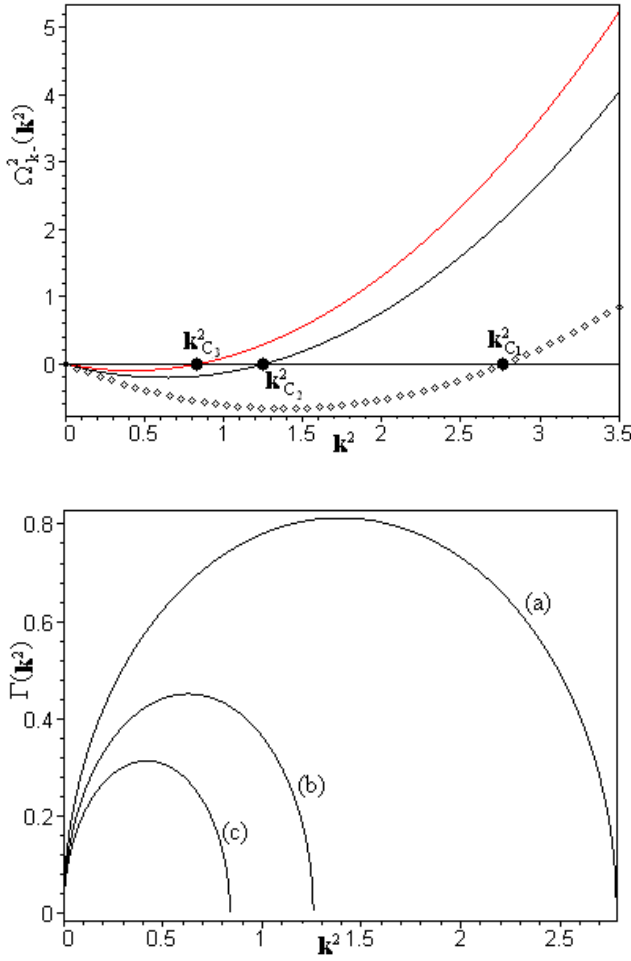


FIG. 5. (Color online) The perturbation square frequency Ω_k^2 (a) and the typical structure of the modulational instability growth rate Γ (b) as a functions of squared modulation wave number k^2 in the special case when $k_B^{X_0} = -k_A^{X_0} = -0.4$, $k_B^{Y_0} = -k_A^{Y_0} = -0.2$, and the line parameters $L = 200 \mu\text{H}$, $V_0 = 2 \text{ V}$, and $C_0 = 370 \text{ pF}$. (a) The dotted black curve, the solid black curve, and the solid red curve correspond to $C_S = 0, 50$, and 100 pF , respectively. (b) Curves *a*, *b*, and *c* correspond to $C_S = 0, 50$, and 100 pF , respectively. The region of the modulational instability and the values of the modulational instability growth rate Γ decrease with the introduction of the linear capacitance $C_S = 0$.

100 pF , respectively. Each square frequency shown in Fig. 5(a) admits both negative and positive values. The values of k^2 for which the negative values are taken correspond to the modulational instability wave numbers. The value of k^2 for which these curves cross zero are the critical wave numbers; they are $k_{C_1}^2 \approx 2.7854$, $k_{C_2}^2 \approx 1.2578$, and $k_{C_3}^2 \approx 0.83802$. Figure 5(b) gives the modulational instability growth versus k^2 . For Fig. 5(b), curves *a*, *b*, and *c* of correspond to $C_S = 0, 50$, and $C_S = 100 \text{ pF}$, respectively, and are depicted for $0 \leq k^2 \leq k_{C_j}^2$, $j = 1, 2, 3$. Figures 5(a) and 5(b) show that the region of the modulational instability and the values of the modulational instability growth rate Γ decrease with the introduction of the linear capacitance $C_S = 0$. We can then conclude that the effect of dispersive element C_S is to decrease the instability region and the instability growth rate.

In Fig. 6, we plot the electrical amplitudes $|\psi_j(x, y, \tau)|$ ($j = 1, 2$) of the perturbed Stokes wave solutions of system (8) for different times. We have used the modulation wave vector $(K, Q) = (0.5, 0)$, which corresponds to the modulation wave number $k = 0.5$. In each of Figs. 6(a)–6(f), the red horizontal line corresponds to the amplitude of the Stokes wave, the solid black curve denotes the electrical amplitude at the initial time $\tau = 0$, and the dotted black line denotes the electrical amplitude for $\tau > 0$. Curves *a*, *c*, and *e* are the amplitude of the component $\psi_1(x, y, \tau)$, while curves *b*, *d*, and *f* are the $\psi_2(x, y, \tau)$ component amplitudes. Figures 6(a)–6(f) correspond to the dispersive element $C_S = 0, 50$, and $C_S = 100 \text{ pF}$, respectively. Curves *b*, which correspond to $C_S = 0$ and $\tau = 63 \times 10^9$, show that the instability is intensified by $\tau = 63 \times 10^9$. Curves correspond to $C_S = 50 \text{ pF}$ and $\tau = 96 \times 10^9$ and show that the instability is observed by $\tau = 96 \times 10^9$. It is seen from curves *f*, which correspond to $C_S = 100 \text{ pF}$ and $\tau = 131 \times 10^9$, that the instability is remarkable from $\tau = 131 \times 10^9$. For time $\tau = 63 \times 10^9$ or $\tau = 96 \times 10^9$, or $\tau = 131 \times 10^9$, at least one of the corresponding $|\psi_1(x, y, \tau)|$ and $|\psi_2(x, y, \tau)|$ is far away from the Stokes wave amplitude $|\psi_{10}|$ or $|\psi_{20}|$. We can then conclude that the introduction of the dispersive element C_S in the electrical line shown in Fig. 2 increases the time over which the onset of instability occurs. This fact is very important. Indeed, as is well known, the instability of a solution does not exclude its observation in experiments: if the time scale over which the onset of instability occurs far exceeds the duration of the experiments, then a formally unstable solution is as relevant for the experiments as is the stable solution.

IV. SUMMARY AND CONCLUSION

Summarizing, we have derived a 2D coupled nonlinear Schrödinger equation to describe the dynamics of nonlinear waves in a discrete nonlinear electrical transmission line with dispersive elements. Exploiting the Stokes wave analysis, we built a result that gives a set of criteria for modulational instability (stability) of plane waves. The criteria of the modulational stability are given by theorems 1 and 2. If one condition of the criteria is not met, then the perturbation frequency develops a finite imaginary part and the solution blows up in time: we say in this case that the plane wave is modulationally unstable. The criteria of modulational instability are given by theorem 3. The computational analysis shows that the effect of dispersive element C_S is to decrease the instability region and the instability growth rate. A few comments and qualitative conclusions should, however, be mentioned.

First, if $V_{11} = V_{22} > 0$, $V_{12} = V_{21}$, and M_1 and M_2 have the same sign, let us say, $M_j < 0$, then we obtain from theorems 1 and 2 that stability of any Stokes wave solution is ensured if $V_{11}^2 > V_{12}^2$. Second, if $V_{12} + V_{21} = 0$, $V_{11} = -V_{22} > 0$, $M_1 < M_2 < 0$, then the analysis of theorem 3 shows that the instability of any Stokes wave solution is ensured if $V_{11}^2 - 2V_{12}^2 > 0$. We then conclude from an analysis of theorems 1, 2, and 3 that Stokes wave solutions can be modulationally stable (unstable) for any perturbation amplitude $|\psi_{j0}|$; that is,

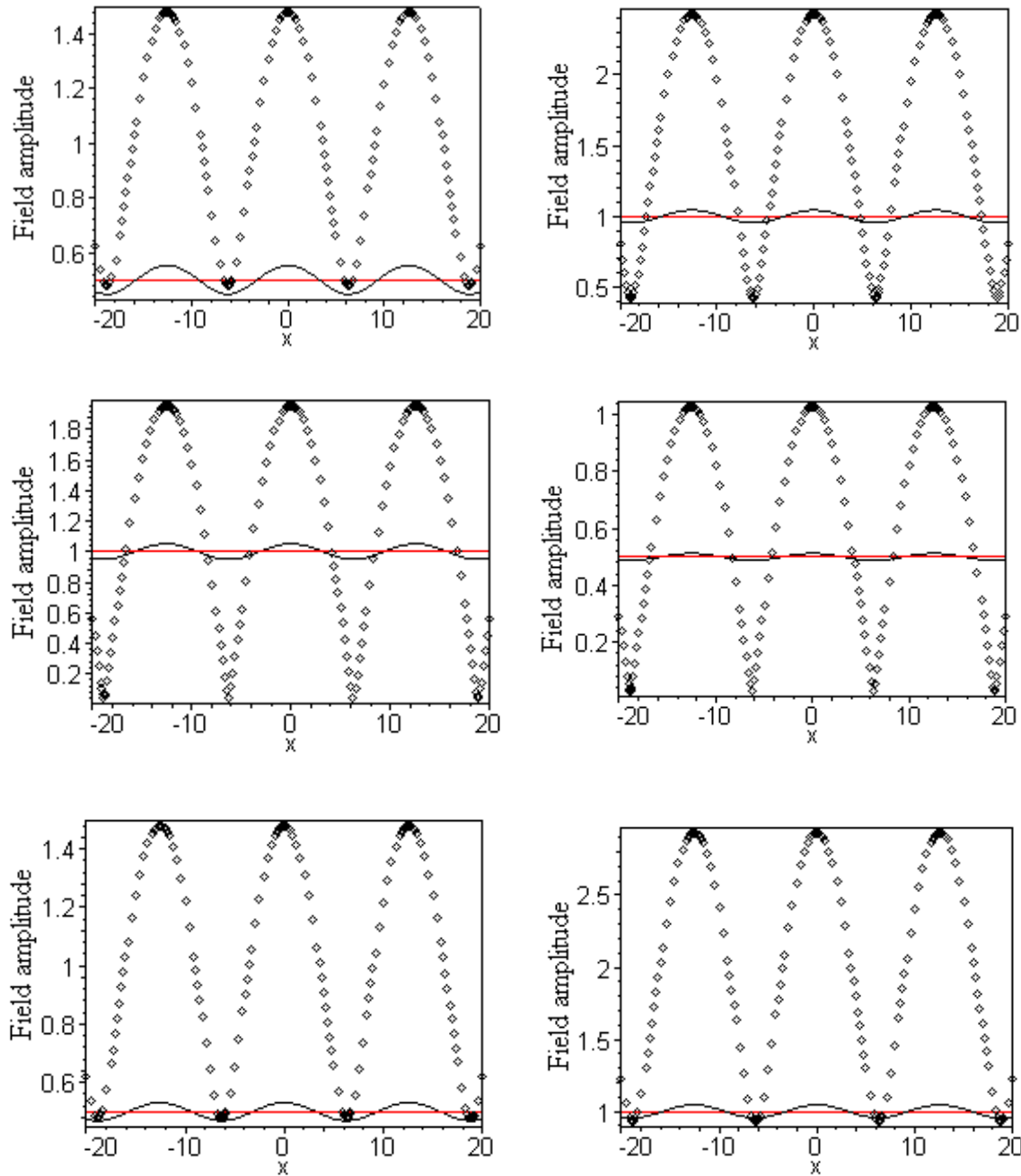


FIG. 6. (Color online) Field amplitudes of perturbed Stokes wave solutions for different time and for $\epsilon=0.01$. The red curve is the Stokes wave amplitude $|\psi_{j0}|$, the solid black curve gives the amplitudes $|\psi_j(x, y, \tau)|$ of the perturbed solution at the initial time $\tau=0$, and the dotted black curve corresponds to the amplitude of the perturbed solution at a given time $\tau > 0$ ($\tau=63 \times 10^9$ for curves *a* and *b* corresponding to $C_S=0$, $\tau=96 \times 10^9$ for curves *c* and *d* that correspond to $C_S=50$ pF, and $\tau=131 \times 10^9$ for curves *e* and *f* for $C_S=100$ pF). The onset of instability occurs at $\tau \approx 96 \times 10^9$, or $\tau \approx 131 \times 10^9$, or $\tau \approx 131 \times 10^9$ for $C_S=0$ or $C_S=50$ pF, or $C_S=100$ pF, respectively.

under some conditions on the coefficients of system (8), any Stokes wave solution $\psi_j = \psi_{j0} \exp[-i(V_{jj}\psi_{j0}^2 + V_{jl}\psi_{3-j0}^2 + \mu_j)\tau]$ is modulationally stable (unstable). These results are also in agreement with that reported in Refs. [44–46] for two-component Bose-Einstein condensate.

The results obtained in this paper are very useful for either the investigation of nonlinear transmission lines or of other similar physical problems, such as nonlinearity, in the plasma, dusty plasma, Bose-Einstein condensates, etc. They

may be helpful in the study of the propagation of two-component solitons on nonlinear transmission lines and other fields of physics.

ACKNOWLEDGMENTS

E.K. acknowledges support provided by the Beijing National Laboratory for Condensed Matter Physics, Institute of Physics, CAS. This work was supported by the NSF of China

under Grants No. 90403034, No. 90406017, No. 60525417, and the National Key Basic Research Special Foundation of China under Grant No. 2005CB724508. We also acknowl-

edge the support from CAS through the project International Team on Superconductivity and Novel Electronic Materials (ITSNEM).

-
- [1] A. B. Aceves, G. G. Luther, C. De Angelis, A. M. Rubenchik, and S. K. Turitsyn, *Phys. Rev. Lett.* **75**, 73 (1995).
- [2] E. Kengne, *Nonlinear Oscillations* **6**, 346 (2003).
- [3] E. Kengne, *J. Phys. A* **37**, 6053 (2004).
- [4] A. C. Newell and J. V. Moloney, *Nonlinear Optics* (Addison-Wesley, New York, 1992).
- [5] F. Abdullaev, S. Darmanyan, and P. Khabibullaev, *Optical Solitons* (Springer-Verlag, Berlin, 1993).
- [6] G. P. Agarwal, *Nonlinear Fiber Optics*, 2nd ed. (Academic Press, New York, 1995).
- [7] A. Hasegawa and Y. Kodama, *Solitons in Optical Communications* (Oxford University Press, Oxford, England, 1995).
- [8] S. Wabnitz, S. Trillo, and E. M. Wright, G. I. Stegeman, *J. Opt. Soc. Am. B* **8**, 602 (1991).
- [9] S. Trillo, S. Wabnitz, W. C. Banyai, N. Finlayson, C. T. Seaton, and G. I. Stegeman, and R. H. Stolen, *IEEE J. Quantum Electron.* **25**, 104 (1989).
- [10] S. V. Manakov, *JETP* **65**, 505 (1973). [*Sov. Phys. JETP* **38**, 248 (1974)].
- [11] D. J. Kaup and B. A. Malomed, *Phys. Rev. A* **48**, 599 (1993).
- [12] M. Karlsson, D. J. Kaup, and B. A. Malomed, *Phys. Rev. E* **54**, 5802 (1996).
- [13] *Nonlinear Klein-Gordon and Schrödinger Systems: Theory and Applications*, edited by L. Vázquez, L. Streit, and V. M. Pérez-Garcá, (World Scientific, Singapore 1997).
- [14] F. Brezzi and P. A. Markowich, *Math. Models Meth. Appl. Sci.* **14**, 35 (1991).
- [15] J. L. López and J. Soler, *Math. Models Meth. Appl. Sci.* **10**, 923 (2000).
- [16] Y. Kivshar and G. P. Agrawal, *Optical Solitons: From Fibers to Photonic Crystals* (Academic Press, New York, 2003).
- [17] A. Hasegawa, *Optical Solitons in Fibers* (Springer-Verlag, Berlin, 1989).
- [18] R. K. Dodd, J. C. Eilbeck, J. D. Gibbon, and H. C. Morris, *Solitons and Nonlinear Wave Equations* (Academic Press, New York, 1982).
- [19] J. L. Rosales and J. L. Sánchez-Gómez, *Phys. Lett. A* **166**, 111 (1992).
- [20] R. Fedele, G. Miele, L. Palumbo, and V. G. Vaccaro, *Phys. Lett. A* **173**, 407 (1993).
- [21] F. Dalfovo, S. Giorgini, L. P. Pitaevskii, and S. Stringari, *Rev. Mod. Phys.* **71**, 463 (1999).
- [22] A. S. Davydov, *Solitons in Molecular Systems* (Reidel, Dordrecht, 1985).
- [23] A. Scott, *Applied and Engineering Mathematics* (Oxford University Press, Oxford, 1999), Vol. 1.
- [24] E. Kengne and W. M. Liu, *Phys. Rev. E* **73**, 026603 (2006).
- [25] E. Timmermans, *Phys. Rev. Lett.* **81**, 5718 (1998).
- [26] Y. B. Band, M. Trippenbach, J. P. Burke, and P. S. Julienne, *Phys. Rev. Lett.* **84**, 5462 (2000).
- [27] D. J. Heinzen, R. Wynar, P. D. Drummond, and K. V. Kheruntsyan, *Phys. Rev. Lett.* **84**, 5029 (2000).
- [28] G.-P. Zheng, J.-Q. Liang, and W. M. Liu, *Phys. Rev. A* **71**, 053608 (2005).
- [29] Z. D. Li, P. B. He, L. Li, J. Q. Liang, and W. M. Liu, *Phys. Rev. A* **71**, 053611 (2005).
- [30] V. A. Brazhnyi and V. V. Konotop, *Phys. Rev. E* **72**, 026616 (2005).
- [31] C. J. Pethick and H. Smith, *Bose-Einstein Condensation in Dilute Gases* (Cambridge University Press, Cambridge, England, 2002).
- [32] Lu Li, Zaidong Li, B. A. Malomed, D. Mihalache, and W. M. Liu, *Phys. Rev. A* **72**, 033611 (2005).
- [33] R. Radhakrishnan and M. Lakshmanan, *J. Phys. A* **28**, 2683 (1995).
- [34] G. B. Whitham, *Proc. R. Soc. London, Ser. A* **283**, 238 (1965).
- [35] T. B. Benjamin and J. E. Feir, *J. Fluid Mech.* **27**, 417 (1967).
- [36] A. Hasegawa, *Phys. Rev. Lett.* **24**, 1165 (1970); T. Taniuti and H. Washimi, *ibid.* **21**, 209 (1968).
- [37] V. I. Karpman and E. M. Krushkal, *Sov. Phys. JETP* **28**, 277 (1969).
- [38] K. Tai, A. Hasegawa, and A. Tomita, *Phys. Rev. Lett.* **56**, 135 (1986).
- [39] L. Salasnich, A. Parola, and L. Reatto, *Phys. Rev. Lett.* **91**, 080405 (2003).
- [40] G. P. Agrawal, *Nonlinear Fiber Optics* (Academic Press, San Diego, 2001).
- [41] J. E. Rothenberg, *Phys. Rev. Lett.* **64**, 813 (1990).
- [42] P. Drummond, T. Kennedy, and J. Dudley, *Opt. Commun.* **78**, 137 (1990).
- [43] F. B. Pelap, T. C. Kofané, N. Flytzanis, and M. Remoissenet, *J. Phys. Soc. Jpn.* **70**, 2568 (2001).
- [44] K. Kasamatsu and M. Tsubota, *Phys. Rev. Lett.* **93**, 100402 (2004).
- [45] T. S. Raju, P. K. Panigrahi, and K. Porsezian, *Phys. Rev. A* **71**, 035601 (2005).
- [46] I. Kourakis, P. K. Shukla, M. Marklund, and L. Stenflo, *Eur. Phys. J. B* **46**, 381 (2005).
- [47] N. G. Berloff, *Phys. Rev. Lett.* **94**, 120401 (2005).